

Defect Self-Annihilation in Surfactant-Mediated Epitaxial Growth

M. Horn-von Hoegen,^(a) F. K. LeGoues, M. Copel, M. C. Reuter, and R. M. Tromp

IBM Research Division, Thomas J. Watson Research Center, P.O. Box 218, Yorktown Heights, New York 10598

(Received 26 December 1990)

Islanding and misfit relaxation are obstacles for growth of heteroepitaxial films. Surfactants not only inhibit islanding, but also control defect structure. Growth of Ge on Si(111) was mediated by a monolayer of Sb floating on the surface. Upon exceeding the critical thickness, Shockley partial dislocations initially thread to the surface and then act as nucleation sites for complementary partial dislocations which glide down to the interface, leaving behind a fully relaxed, defect-free, epitaxial Ge film. Thus, the seemingly incompatible goals of strain relief and defect-free growth can be met by a surfactant-modified growth front.

PACS numbers: 61.16.Fk, 68.35.Bs, 68.55.-a

Growth of epitaxial lattice-mismatched films is a crucial challenge in materials science. The benefits of defect-free heteroepitaxial films in semiconductor technology are numerous [1]. For thin films, if layer by layer growth is achieved, a pseudomorphic, strained heterolayer can be grown. For thicker films the strain is relieved by the introduction of defects, which may have a disastrous effect on the transport properties. In many cases these defects "thread" through the film and cannot be overgrown. In general, layer-by-layer growth does not occur, but islanding (Volmer-Weber) or layer-by-layer growth followed by islanding (Stranski-Krastanov) is found, giving rise to discontinuous films [2]. It was shown recently that the growth mode can be changed from islanding to layer by layer by introducing a third element as surfactant [3,4]. In this Letter we show that use of a surfactant may also allow control of the defect structure above the critical thickness. In particular, we find that threading defects introduced during the initial phase of strain relief self-annihilate upon continued growth, leaving behind a dislocation network at the Si-Ge interface. No defects are observed in the bulk of the Ge film.

The driving force for the formation of dislocations is the strain energy built up by the lattice mismatch between the substrate and overlayer. In the Si-Ge system the initial small islands are dislocation free [5,6], but with increasing thickness, dislocations are introduced from the edges of the islands. For thick films, where the islands coalesce, many defects thread up to the surface and cannot be overgrown.

Changing the growth mode to layer by layer also changes the conditions for introducing defects. For growth of Ge on Si(001) with an As surfactant, a so-called V-shaped defect has been observed, which in most cases cannot be overgrown [6,7]. In this Letter we show that Sb acts as a surfactant for Ge growth on Si(111), stabilizing layer-by-layer growth instead of the Stranski-Krastanov mode. In addition, the Sb monolayer drastically modifies defect introduction. At a Ge thickness of 8–10 monolayers [1 monolayer (ML) = 7.8×10^{14} atoms/cm²], partial dislocations glide from the surface to the interface. But the partial dislocation is still topologically joined to the surface by a stacking fault that threads

through the Ge film. This stacking fault acts as the nucleation site for a complementary partial dislocation, which annihilates the defect extending to the surface and leaves a full, but split dislocation at the interface. The resulting Ge film is fully strain relieved and defect free with all dislocations confined to the Si-Ge interface.

Sb changes the surface properties and reduces the chemical reactivity by passivating the Si or Ge surface dangling bonds. It forms a $(\sqrt{3} \times \sqrt{3})R30^\circ$ reconstruction on Si(111) [8,9] and a (2×1) reconstruction on Ge(111). In the $(\sqrt{3} \times \sqrt{3})$ structure the Sb atoms form trimers, with each Sb atom bonded with one electron to a Si top atom and with two electrons to the two neighboring Sb atoms. The remaining two electrons form a lone pair orbital. On Ge(111) the Sb forms zigzag chains running in the $[1\bar{1}0]$ direction [10]. The Sb is similarly bonded as on Si(111), passivating the Ge dangling bonds. The surface free energy of Sb-covered Ge and Si surfaces is lowered due to this energetically favored filling of dangling bonds.

Experimental results were obtained by *in situ* examination with medium-energy ion scattering (MEIS), low-energy electron diffraction (LEED), *ex situ* high-resolution cross-sectional transmission electron microscopy (TEM), and Raman scattering. The samples were prepared under ultrahigh-vacuum conditions in a molecular-beam-epitaxy (MBE) chamber directly coupled to the MEIS chamber with facilities for x-ray photoelectron spectroscopy (XPS). The MEIS system has been described in detail [11] and a review of the experimental technique can be found in the literature [12]. Channeling data were taken with 200-keV He⁺ ions incident in the $[00\bar{1}]$ direction and the detector positioned along the $[1\bar{1}\bar{1}]$ blocking direction. Random spectra were obtained by an azimuthal rotation of 7.7° about the sample normal and a polar rotation of 4°.

High-resolution cross-sectional TEM samples were prepared by mechanical thinning to $\sim 30 \mu\text{m}$ followed by liquid-nitrogen- (LN₂-) cooled ion milling to electron transparency. The samples were observed in a JEOL 4000 electron microscope operating at 400 keV.

Clean Si(111) samples (SEH, *n* type, 10 mΩ cm) were prepared by degassing followed by mild sputtering and a

short flash to 1050°C to remove the native oxide [13]. Deposition took place at a sample temperature of 610°C, with a Ge growth rate of ≈ 1 ML/min. Prior to growth the surface was passivated by saturation with 1-ML Sb, and a small flux of Sb was maintained during growth to avoid Sb depletion.

Evidence of effectiveness of Sb as a surfactant may be seen in the growth of Ge on Si(111). Initial studies were done without Sb: In Fig. 1(a) we show backscattering spectra after deposition of 10-ML Ge at 610°C. The random spectrum (dotted line) shows a peak at 187 keV, due to the 3-ML-thick continuous Ge film (Stranski-Krastanov layer) covering the entire surface. The long low-energy tail is caused by Ge islands, with an average island height of about 50 ML, covering $\approx 15\%$ of the surface. The Si substrate gives rise to the scattering intensity below 173 keV. Because of shadowing of the subsur-

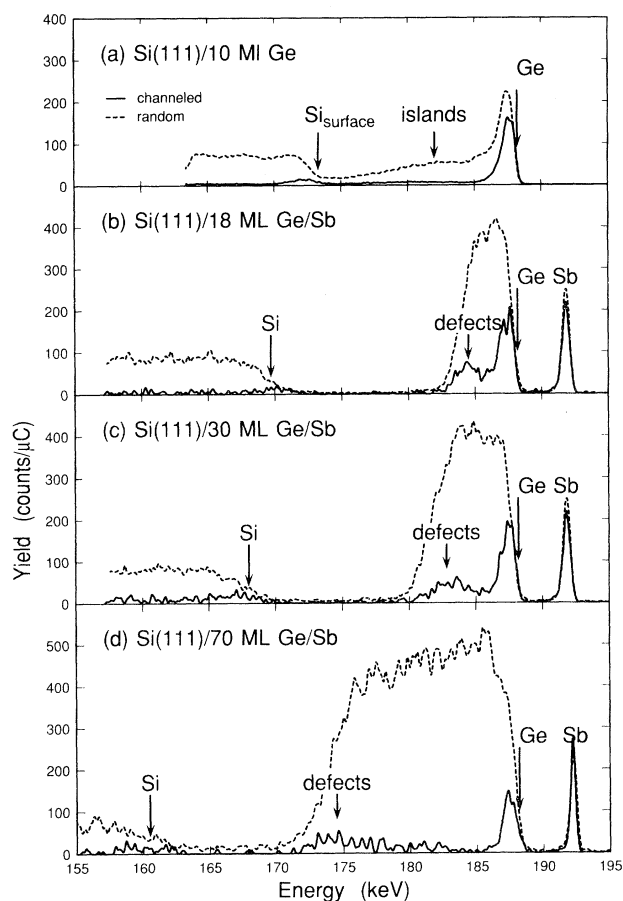


FIG. 1. Ion backscattering spectra for Ge films grown at 61°C. Both random and channeling spectra are shown. (a) Growth without surfactant results in islanding after ≈ 3 ML of Ge, indicated by the low-energy tail of the Ge peak. (b)–(d) Ge films grown with Sb as a surfactant show no sign of islanding. The channeling spectra show the peak due to dislocations at the Ge-Si interface. The Si signal is shifted to lower values due to the Ge film thickness.

face atoms only the Ge surface peak at 187 keV is seen in the channeling spectrum (solid line). Threading defects and dislocations in the Ge islands produce the slight rise in background below 185 keV.

Ge films grown with an Sb saturated surface show an altogether different behavior. In Figs. 1(b)–1(d) we show backscattering spectra for 18-, 30-, and 70-ML-thick Ge films on Si(111). The random spectra always show a compact trapezoidal shape for the Ge yield, reflecting a continuous, uniformly thick film. Electronic energy losses in the Ge film, adding up to the full width at half maximum of the Ge signal, shift the Si substrate signal to lower values. The channeling spectra show two features: the Ge surface peak at 187 keV, and another peak at the low-energy edge of the Ge signal (the Si-Ge interface), found in films grown past the critical thickness for defect introduction. The integral yield of the interface peak corresponds to 2 ML of Ge, independent of film thickness. The peak does, however, broaden with increasing film thickness, as a result of the energy straggling of the ions. We will show later that this peak is correlated with dislocations at the interface.

To investigate the crystal quality in more detail, we determined the minimum yield (χ_{\min}) of the Ge films, defined as the ratio of the intensity in channeling geometry to that in random geometry. In Fig. 2 the solid triangles show χ_{\min} for the Ge signal below 185 keV [excluding the Ge surface peak, see inset (b) in Fig. 2]. The strong decrease of χ_{\min} with increasing film thickness indicates an increasing defect-free region in the film. As mentioned above, the strain-relief defects at the Si-Ge interface result in a scattering intensity equivalent to 2 ML

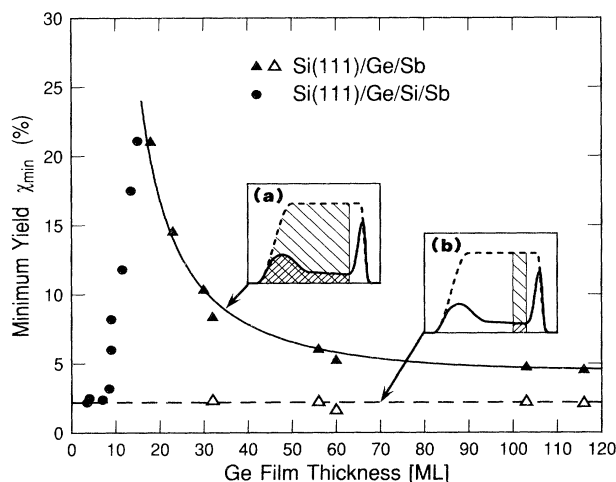


FIG. 2. The minimum yield (χ_{\min}) as a function of Ge film thickness. The region between the Ge surface peak and the Ge-Si interface exhibits a yield comparable to a bulk Ge crystal. \blacktriangle : including interface, as shown in inset (a); \triangle : excluding interface, as shown in inset (b); \bullet : embedded Ge film (from Ref. [3]); —: model described in the text.

of Ge. With increasing Ge coverage (θ) the interface contributes less and less to χ_{\min} , which asymptotically approaches 2.2%. The solid line in Fig. 2 is based on a model assuming a constant contribution of 2 ML to the χ_{\min} of a Ge(111) crystal:

$$\chi_{\min} = \chi_{\min, \text{Ge}(111)} + (2 \text{ ML})/\theta.$$

If the interface region is excluded from the calculation of χ_{\min} (open triangles), then a low value is obtained, $\chi_{\min} \approx 2.2\%$, indicating a high-quality film.

Measurements for thinner Ge films [14] clearly show the onset of defect formation for Ge films exceeding the critical thickness of 8 ML (solid circles in Fig. 2). These Ge films are embedded in Si to avoid the occurrence of a Ge surface peak, which would dominate the spectra. Note that the initial low minimum yield of $\approx 2.2\%$ for the defect-free strained films is the same as shown with the open triangles.

For the thick Ge films the angular positions of the blocking minima are the same for the Ge film and for the Si substrate, indicating that the Ge is fully strain relieved. Raman-scattering measurements show an unshifted Ge phonon, characteristic of unstrained Ge, without any intermixing with Si. The peak broadening of 3 cm^{-1} of this phonon is the same as expected for a Ge(111) crystal with a doping concentration of $\approx 3 \times 10^{19}/\text{cm}^3$. Based on ion-scattering data we estimate an upper limit of incorporation of $\approx 4 \times 10^{19} \text{ Sb}/\text{cm}^3$.

Low-energy electron diffraction of the (2×1) reconstructed Ge surface also reflects excellent epitaxial quality of the Ge films. We observe sharp, brilliant spots with a low background, indicating large superstructure domains, no terraces, and excellent crystal quality (within the resolution limit of 100 \AA).

High-resolution cross-sectional TEM was used to determine the nature, structure, and location of the strain-relieving defects as a function of film thickness. The strain relief occurs in two stages. First, a Shockley partial dislocation (SPD) [15] nucleates at the surface, glides down to the interface, and cross slips laterally along the interface [Fig. 3(a)], leaving behind stacking faults in the film and at the interface. In the second state of strain relief—at somewhat larger thickness—a second SPD is nucleated at the surface and glides to the interface, eliminating the portion of the stacking fault that threads through the epilayer. Additionally, an edge dislocation climbs from the interface to the surface, removing a Ge(111) double layer from the film. Figure 3(b) shows a 70-ML film. The bulk of the film is now perfect. Since the misfit is entirely relieved by SPD's, the interface is composed of alternating faulted and unfaulted regions, clearly seen in Fig. 3(b).

In detail, the following reactions take place to achieve strain relief. A full interfacial $\frac{1}{2} [10\bar{1}]$ dislocation, glissile on (11), can be decomposed into a $\frac{1}{2} [0\bar{1}\bar{1}]$ dislocation, glissile on the $(11\bar{1})$ plane, and a $\frac{1}{2} [110]$ sessile

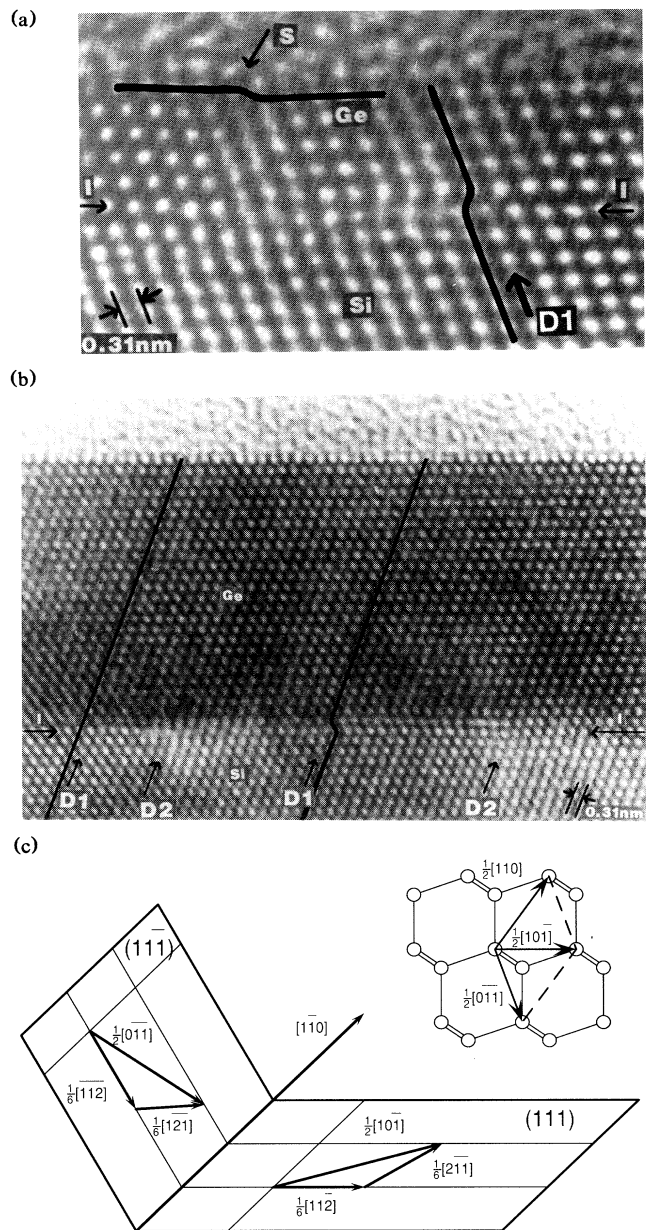


FIG. 3. Cross-sectional transmission electron micrographs of Ge/Si(111) at various stages of growth. (a) A 10-ML Ge film showing a partial dislocation ($D1$) located at the Si-Ge interface (I). A stacking fault extends along the interface, then threads towards the surface (S). (b) A 70-ML Ge film with fully evolved microstructure. The interface (I) contains a network of Shockley partial dislocations, ($D1$) and ($D2$) (see text). Threading dislocations are completely absent from the bulk of the Ge film. (c) Dislocation decomposition diagrams (see text).

edge dislocation [Fig. 3(c)]. In addition, the $\frac{1}{2} [0\bar{1}\bar{1}]$ and $\frac{1}{2} [10\bar{1}]$ dislocations can each be dissociated into two SPD's as follows: $\frac{1}{2} [0\bar{1}\bar{1}] = \frac{1}{6} [\bar{1}\bar{1}\bar{2}] + \frac{1}{6} [1\bar{2}\bar{1}]$ and $\frac{1}{2} [10\bar{1}] = \frac{1}{6} [11\bar{2}] (D1) + \frac{1}{6} [2\bar{1}\bar{1}] (D2)$ [Fig. 3(c)]. First,

a glissile $\frac{1}{6} [\bar{1}\bar{1}\bar{2}]$ SPD is injected onto the $(11\bar{1})$ plane as a half loop from the surface. This dislocation has a significant component in the (111) plane to relieve some of the strain. It glides down and then cross slips onto the interface to form a $\frac{1}{6} [11\bar{2}]$ SPD [D1, Figs. 3(a) and 3(b)], distributing the strain relief over a larger area along the interface. Both SPD's leave a stacking fault behind them, easily recognized in Fig. 3(a). In addition, a so-called stair-rod dislocation is formed where the two stacking faults intersect, with Burgers vector $\frac{1}{6} [\bar{1}\bar{1}\bar{2}] - \frac{1}{6} [11\bar{2}] = \frac{1}{6} [\bar{2}\bar{2}0]$. Next, a $\frac{1}{6} [1\bar{2}\bar{1}]$ SPD nucleates on the stacking fault threading to the surface. Added to the first SPD on this plane it forms the full $\frac{1}{2} [0\bar{1}\bar{1}]$ dislocation and annihilates the stacking fault as it glides to the interface. Like the first SPD, $\frac{1}{6} [1\bar{2}\bar{1}]$ cross slips onto the interface to form $\frac{1}{6} [2\bar{1}\bar{1}]$ (D1). Again, a stair-rod dislocation is formed with Burgers vector $\frac{1}{6} [1\bar{2}\bar{1}] - \frac{1}{6} [2\bar{1}\bar{1}] = \frac{1}{6} [\bar{1}\bar{1}0]$. This reacts with the already present stair-rod dislocation: $\frac{1}{6} [\bar{1}\bar{1}0] + \frac{1}{6} [\bar{2}\bar{2}0] = \frac{1}{2} [\bar{1}\bar{1}0]$, i.e., the required edge dislocation. Finally, the $\frac{1}{2} [\bar{1}\bar{1}0]$ edge dislocation climbs to the nearby surface, removing a full $(11\bar{1})$ double layer from the Ge film, adding greatly to the strain relief. That this $\frac{1}{2} [\bar{1}\bar{1}0]$ edge dislocation is mobile at 610°C was shown previously during growth of Ge on Si(001), where such dislocations were found to climb in the Si host at temperatures as low as 500°C .

While this process may seem unlikely and unduly complicated, it reflects the difficulty in nucleating the required dislocations. To nucleate the $\frac{1}{2} [10\bar{1}]$ dislocation directly at the interface would be impossible since there is no source. On the other hand, nucleating in one step both $\frac{1}{2} [0\bar{1}\bar{1}]$ and $\frac{1}{2} [110]$ dislocations would be difficult due to the high formation energies of these defects. However, the $\frac{1}{2} [0\bar{1}\bar{1}]$ dislocation is easily dissociated into two SPD's with lower formation energy. The edge dislocation is generated in two steps also, and the final interfacial dislocation is dissociated into two SPD's, lowering the formation energies for these defects as well. Thus, the system manages to inject two easily nucleated SPD's from the surface—and achieve full strain relief. On the average, one full dislocation is observed every 25 lattice fringes, thus relieving the misfit completely.

The annihilation of the threading portion of the dislocation is an extremely efficient process. It has been observed in a large number of cross-sectional samples, with a *total* absence of threading defects such as stacking faults and screw dislocations. From these observations we conclude that the number of threading defects is smaller than $10^8/\text{cm}^2$. In contrast, defect densities for structures grown by conventional procedures suffer from defect densities as high as $10^{12}/\text{cm}^2$. In addition, the dislocation network is remarkably abrupt in the growth direction. If we neglect the strain fields, the dislocations

are localized to within a few atomic planes of the interface.

Epitaxial growth of non-lattice-matched structures is a struggle to simultaneously control film morphology, strain relief, and defect structure. Conventional growth strategies may include the use of thick buffer layers and even superlattices to relieve lattice mismatch and to exclude defects from the active regions. Control of surface free energy with a surfactant eliminates islanding. Simultaneously, it strongly modifies defect nucleation as a direct consequence of forcing layer-by-layer growth. For Ge on Si(111), the defect microstructure is *self-annihilating*, since each thread contains the seeds of its own destruction. The result is an ideal heterostructure, consisting of two perfect, fully relaxed crystals joined at an atomically abrupt interface.

We would like to acknowledge discussions with J. Tsang, and wish to thank him for Raman-scattering measurements.

^(a)Present address: Institut für Festkörperphysik, Universität Hannover, Appelstrasse 2, 3000 Hannover 1, Federal Republic of Germany.

- [1] D. W. Goodman, in *Heterostructures on Silicon: One Step Further with Silicon*, edited by Y. I. Nissim and E. Rosencher (Kluwer, Dordrecht, 1989).
- [2] P. M. Marée, K. Nakagawa, F. M. Mulders, and J. F. van der Veen, *Surf. Sci.* **191**, 305 (1987).
- [3] M. Copel, M. C. Reuter, E. Kaxiras, and R. M. Tromp, *Phys. Rev. Lett.* **63**, 632 (1989).
- [4] M. Copel, M. C. Reuter, M. Horn-von Hoegen, and R. M. Tromp, *Phys. Rev. B* **42**, 11 682 (1990).
- [5] D. Eaglesham and M. Cerullo, *Phys. Rev. Lett.* **64**, 1943 (1990).
- [6] F. K. LeGoues, M. Copel, and R. M. Tromp, *Phys. Rev. B* **42**, 11 690 (1990).
- [7] F. K. LeGoues, M. Copel, and R. M. Tromp, *Phys. Rev. Lett.* **63**, 1826 (1989).
- [8] C. Park, T. Abukawa, T. Kinochita, Y. Enta, and S. Kono, *Jpn. J. Appl. Phys.* **27**, 147 (1988).
- [9] P. Mårtensson, G. Meyer, N. M. Amer, E. Kaxiras, and K. C. Pandey, *Phys. Rev. B* **42**, 7230 (1990).
- [10] G. Meyer and B. Voigtlaender (to be published).
- [11] R. M. Tromp, H. H. Kersten, E. Granneman, F. W. Saris, R. J. Koudjjs, and W. J. Kilsdonk, *Nucl. Instrum. Methods Phys. Res., Sect. B* **232**, 155 (1984).
- [12] J. F. van der Veen, *Surf. Sci. Rep.* **5**, 199 (1985).
- [13] M. Copel and R. M. Tromp, *Phys. Rev. B* **37**, 2766 (1988).
- [14] M. Horn-von Hoegen, M. Copel, M. Reuter, and R. M. Tromp (to be published).
- [15] J. Hirth and J. Lothe, *Theory of Dislocations* (Wiley, New York, 1982).

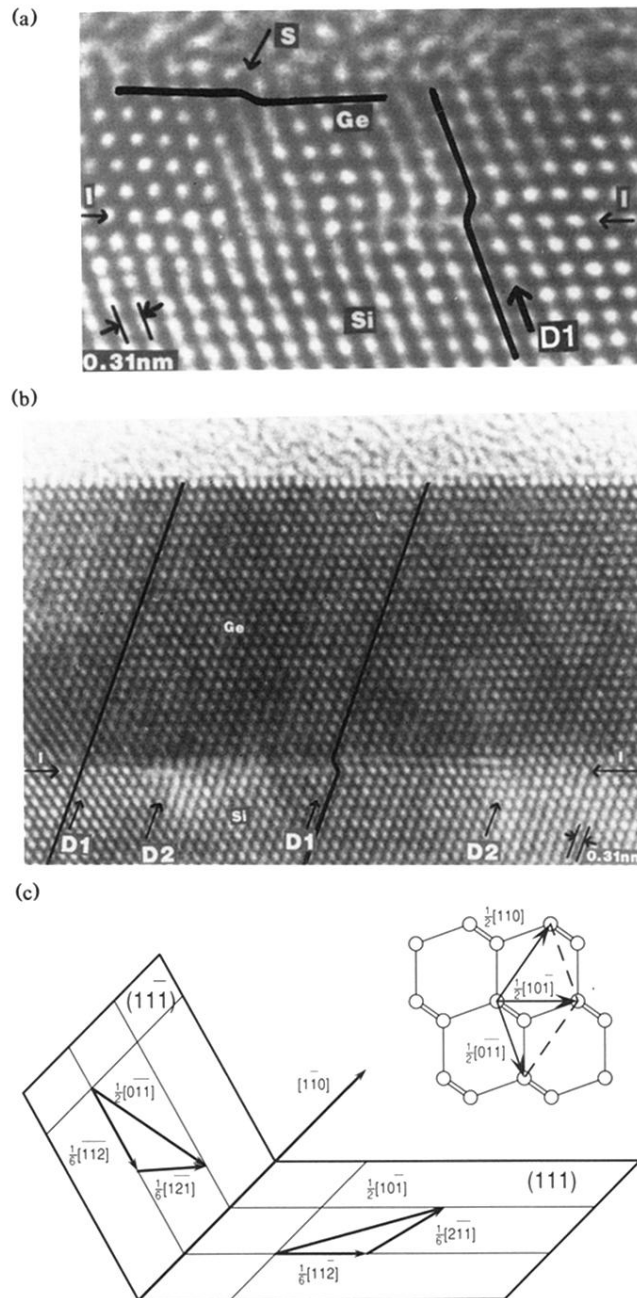


FIG. 3. Cross-sectional transmission electron micrographs of Ge/Si(111) at various stages of growth. (a) A 10-ML Ge film showing a partial dislocation ($D1$) located at the Si-Ge interface (I). A stacking fault extends along the interface, then threads towards the surface (S). (b) A 70-ML Ge film with fully evolved microstructure. The interface (I) contains a network of Shockley partial dislocations, ($D1$) and ($D2$) (see text). Threading dislocations are completely absent from the bulk of the Ge film. (c) Dislocation decomposition diagrams (see text).